PERGAMON

Computers and Structures 79 (2001) 1077–1088

Computers & Structures

www.elsevier.com/locate/compstruc

Design, modelling and analysis of a six component force balance for hypervelocity wind tunnel testing

A.L. Smith [a], D.J. Mee [a,*], W.J.T. Daniel [a], T. Shimoda [b]

[a] *Department of Mechanical Engineering, The University of Queensland, Brisbane QLD 4072, Australia*
[b] *Tsukuba Space Centre, 2-1-1 Sengen, Tsukuba City, Ibaraki 305, Japan*

Received 15 October 1999; accepted 26 October 2000

Abstract

A combination of modelling and analysis techniques was used to design a six component force balance. The balance was designed specifically for the measurement of impulsive aerodynamic forces and moments characteristic of hypervelocity shock tunnel testing using the stress wave force measurement technique. Aerodynamic modelling was used to estimate the magnitude and distribution of forces and finite element modelling to determine the mechanical response of proposed balance designs. Simulation of balance performance was based on aerodynamic loads and mechanical responses using convolution techniques. Deconvolution was then used to assess balance performance and to guide further design modifications leading to the final balance design.

Keywords: Force balance design; Force measurement; Finite element modelling; Deconvolution; Shock tunnel; Hypersonic

1. Introduction

Force measurement techniques in wind tunnel testing are necessary for determining a variety of aerodynamic performance parameters. These parameters are used to assess the aerodynamic characteristics of a vehicle and to guide further design refinements. Typically these techniques rely on static measurement of the reaction forces produced in the model support structure and are designed to minimize *balance interactions* [1], or coupling between the outputs. This type of measurement technique is used routinely in wind tunnels where the test period is of the order of hundreds of milliseconds to hours.

Hypervelocity aerodynamic testing is typically conducted using impulse-type wind tunnel facilities. These facilities are capable of producing the high enthalpy flows necessary for aerodynamic simulation but are limited by the duration of the test flow. The typical test flow duration of a reflected shock tunnel is between one and three milliseconds. Consequently, techniques which rely on static measurement of the reaction forces produced in the model support, cannot be used. This is because there is insufficient time for the transient vibrations arising from the loading to decay to an acceptable level.

One force measurement technique which has been found to overcome the limitations associated with short test times is the *stress wave force measurement technique*. This technique was originally proposed by Sanderson and Simmons [2] and relies on measuring and interpreting the stress waves which propagate within a model and its support as a result of aerodynamic loading. Since its development, Daniel and Mee [3] have extended the technique through finite element modelling of two and three component balance designs. This lead to the development of a three component balance which permitted the measurement of lift force, drag force and pitching moments on a short conical model in a reflected shock tunnel [4].

* Corresponding author. Tel.: +61-7-3365-4058; fax: +61-7-3365-4799.
E-mail address: mee@mech.uq.edu.au (D.J. Mee).

0045-7949/01/$ - see front matter
PII: S0045-7949(01)00005-0

This paper extends the modelling work of Daniel and Mee [3] and demonstrates how a number of modelling techniques can be combined to simulate the performance of a six component stress wave force balance. The simulated performance is used to optimism the balance design for both measurement flexibility and accuracy, whilst subject to the testing constraints of a hypervelocity shock tunnel facility. The aerodynamic loads on the proposed test model were estimated using a numerical flow solver. Finite element modelling was used to characterize the relationship between the applied model loads and the subsequent mechanical response of the balance structure. The test model and balance were modelled as a linear dynamic system in which the response of the balance to applied loads could be determined using numerical convolution and superposition. The response was assessed using a numerical deconvolution technique which enabled the dynamic behaviour of balance designs to be evaluated for a typical shock tunnel aerodynamic loading time history. Results from this evaluation were then used to guide improvements in the overall balance design in order to optimize the measurement capability.

The motivation for this study is to understand the design limitations and to improve the accuracy of the stress wave force measurement technique, especially in resolving lift force, drag force and pitching moment components. The application for the present design is the development of a six component balance for aerodynamic force measurement on a scaled model of the HYFLEX vehicle. HYFLEX [5], the HYpersonic FLight EXperiment, was developed by NAL/NASDA of Japan and was tested in February 1996. HYFLEX was a blunt-nosed hypersonic vehicle which separated from a J-1 rocket at Mach 15 at an altitude of 110 km. Its descent was then controlled through aerodynamic braking.

2. Force measurement technique

The stress wave force measurement technique relies on characterizing the dynamic response of the wind tunnel model and its support. Although the technique permits the simultaneous measurement of single and multiple force components, here the underlying principles are introduced for a single component force balance.

The single component stress wave force balance is essentially a variation of the original Hopkinson pressure bar experiment [6] and consists of a model rigidly connected to an elastic stress bar. The stress bar serves as the model support and the arrangement is suspended in the flow so that there is no restriction to movement in the flow direction. The impulsive aerodynamic loading on the model causes stress waves to propagate within the model. These waves reflect within the model and are progressively transmitted into the supporting stress bar. By treating the dynamic behaviour of this arrangement as a linear system, the time history of strain in the supporting stress bar can be described using a convolution integral,

$$y(t) = \int_0^t g(t-\tau)u(\tau)\,\mathrm{d}\tau. \tag{1}$$

Here $u(t)$ is the input to the system (aerodynamic drag force on the model), $y(t)$ is the resulting output (measured strain time history in the supporting stress bar) and $g(t)$ is an impulse response function. The impulse response function describes the relationship between the system input and output. When the data are discretised Eq. (1) can be re-written using matrix notation,

$$y = Gu, \tag{2}$$

where u and y are vectors for the discretised input and output signals and G is a square matrix formed from the discretised impulse response.

To implement this technique experimentally, the unknown aerodynamic drag force on the model is determined from solution of Eq. (2) using the measured strain time history and by knowing the impulse response function of the system (determined experimentally or numerically). Thus the problem becomes an inverse one and the drag force can be found using a numerical deconvolution procedure.

To extend the stress wave force measurement technique to multiple components, there must be at least as many measured outputs as there are unknown inputs. Ideally each of the outputs would be independently related to an input which would make the system completely decoupled. In this situation each component could be treated separately using deconvolution. Although force balance design generally attempts to minimize coupling, in practice some coupling is always present between the individual components. For instance, in a balance designed to measure lift force, drag force and pitching moment, a pure drag force acting on the model may produce a signal primarily on the drag force output, but may also produce a signal on the other two outputs. This presents a problem for the accurate measurement of all components, but can be overcome by determining the impulse responses for all the outputs subject to all the inputs. In this way a complete description of the system is obtained and can be written in matrix form for n-components as,

$$\begin{pmatrix} y_1 \\ y_2 \\ \vdots \\ y_n \end{pmatrix} = \begin{bmatrix} G_{11} & G_{12} & \cdots & G_{1n} \\ G_{21} & G_{22} & \cdots & G_{2n} \\ \vdots & \vdots & \ddots & \vdots \\ G_{n1} & G_{n2} & \cdots & G_{nn} \end{bmatrix} \begin{pmatrix} u_1 \\ u_2 \\ \vdots \\ u_n \end{pmatrix}, \tag{3}$$

where u_i and y_i are vectors of the system inputs and outputs, assembled sequentially and G_{ij} contains the

impulse responses from the individual component sub-matrices, as per Eq. (2). The off-diagonal sub-matrices in Eq. (3) represent coupling between the outputs and are generally undesirable.

In the present study the solution to Eq. (3) was determined using a time domain deconvolution program, developed by Mee [7], for up to six-dimensional coupled problems. The basis for this program is an algorithm suggested by Prost and Goutte [8] which uses functional minimization with the extended conjugate gradient algorithm.

3. Aerodynamic modelling

Aerodynamic modelling was used to estimate the distribution of force and the location of the centre of pressure on the HYFLEX vehicle. For this modelling a flow solver, based on modified-Newtonian flow theory [9], was used. Newtonian modelling is a simple way of estimating pressure coefficients on objects in hypersonic flows. The pressure coefficient depends only on the local inclination of the surface to the oncoming flow and on the oncoming flow properties. A fine surface mesh of the model is produced (see Fig. 1) and, for each surface element, the local surface normal direction is compared with the flow direction to determine its angle to the oncoming flow. This allows a pressure for each element to be found. Regions shadowed from the oncoming flow, such as those on the leeward side of the model, are assumed to have a surface pressure equal to that of the free stream. The net forces on the model can then be found by integrating the pressure distribution for all surface elements. Viscous forces are neglected. This type of code was chosen because it is very simple and fast and is capable of providing a good estimate of the pressure distribution on windward surfaces in hypersonic flow [10]. It is particularly well suited to situations where the windward surfaces are relatively blunt [10] and the shape of the bow shock wave is similar to the shape of the surface, as is the case for HYFLEX.

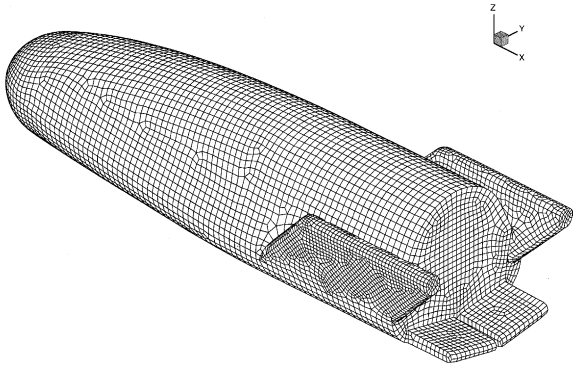

Fig. 1. A typical surface mesh used in conjunction with the Newtonian flow solver to model the aerodynamic loading distribution on a hypersonic vehicle.

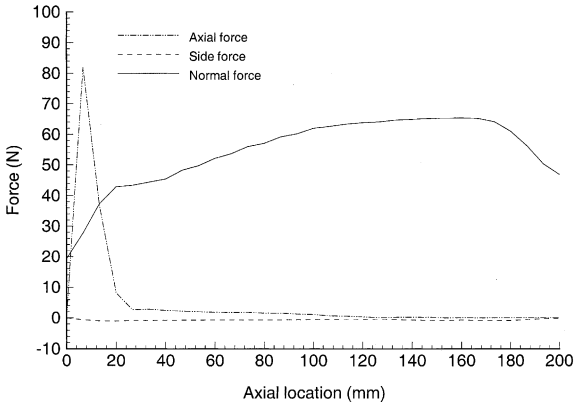

Fig. 2. The axial distribution of aerodynamic forces acting on a model of a hypersonic vehicle.

The distribution of force along the major axis of the test model was estimated for the anticipated model orientation and test flow conditions. This distribution of force is illustrated in Fig. 2 for the axial, side and normal force components. Note that the axial, side and normal directions correspond to the x-, y- and z-axes in Fig. 1.

4. Finite element modelling

Finite element (FE) modelling is used in the design process to analyze the dynamic behaviour of different force balance designs. FE modelling can also be used to provide insight into the nature of coupling between balance outputs and the sensitivity of the design to variations in the loading distribution. FE modelling was used to determine the complete impulse response matrix of Eq. (3) for each balance design. The procedure used is outlined below.

A step change in load was applied to a principal load component, while keeping all other components zero. This produced a step response in all of the balance outputs. The step responses from each of the balance outputs were then differentiated to produce impulse responses for each output. This gave a single row of the impulse response matrix in Eq. (3). This procedure was then repeated for each of the principal force components until the complete impulse response matrix was determined.

All the FE models in the present study were developed using MSC/PATRAN and were analysed using MSC/NASTRAN. Both of these packages were run on a Silicon

Graphics Power Challenge Array with a maximum throughput of 7.2 GigaFLOPS. Although MSC/NASTRAN permits solution of transient linear problems using both modal and direct integration methods, only the later was used because the output was required over a short time and an accurate prediction of the frequency content was required. Mainly hexahedral but some pentahedral elements were used in the FE models. Default $2 \times 2 \times 2$ Gaussian quadrature was used with reduced integration of the shear stiffness terms, corrected with a bubble function. The time step used in integration was typically 1 μs.

Several factors influence the accuracy in computing the dynamic or transient response of a structure using FE modelling. These include; mesh refinement, mesh transitions, internal/structural damping, integration time step and the distribution of applied loads. These issues and others were addressed by Daniel and Mee [3] where similar FE modelling techniques were used. The suggestions made there were used in the present simulations. In that study, the results of FE simulations were compared with experimentally measured strains. Based on the good agreement observed there, this modelling is considered to be suitable for stress wave force balance design. It is noted that balances are always fully calibrated experimentally before being used in wind tunnel tests.

5. Simulation of balance performance

Spatial and temporal loading distributions, typical of testing in a hypervelocity impulse facility, were used to predict balance outputs through Eq. (3). The spatial load distributions were determined from aerodynamic modelling and give the loading vector u_i. The impulse responses, determined through FE modelling, give the matrix G_{ij}. The simulated outputs, y_i were then found by performing the coupled convolution described by Eq. (3). These simulated balance output signals contain information from all the applied loads components.

The performance of a balance design was then evaluated by assessing how well the applied loads could be recovered from these outputs. The assessment of the design was made by performing a coupled deconvolution of the simulated output signals with the impulse responses and comparing the actual and recovered loads.

6. Design objectives and constraints

The present balance was designed chiefly for the measurement of lift force, drag force and pitching moment in a wind tunnel simulation of the HYFLEX vehicle flying through the atmosphere at a high angle of

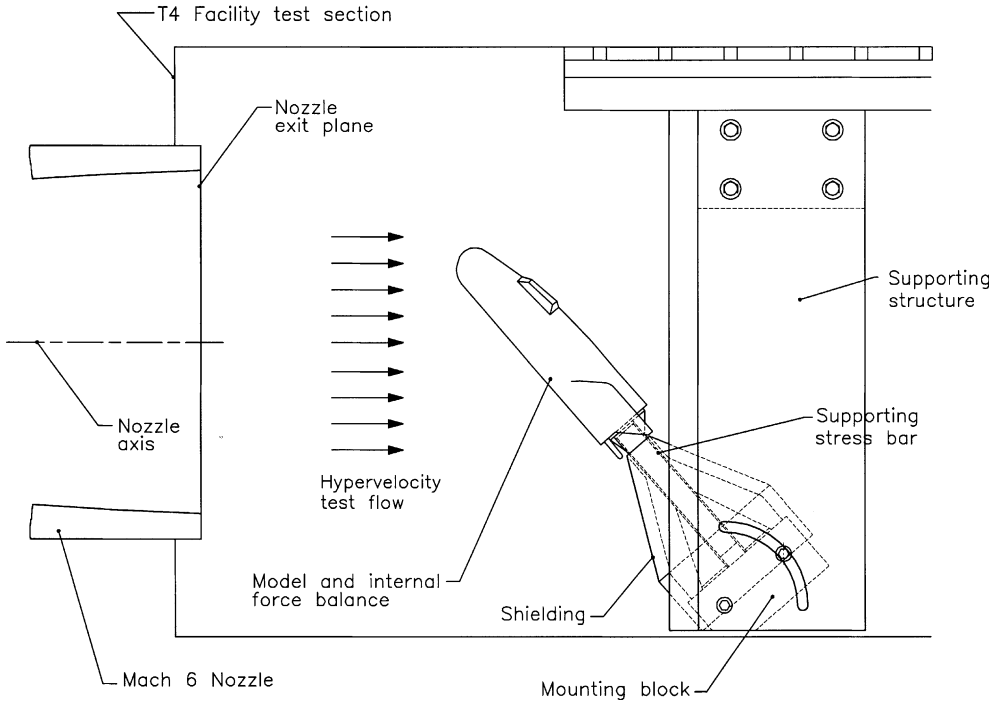

Fig. 3. The general balance configuration and size constraints imposed by the test section of the wind tunnel facility.

attack. These components were of particular interest as they are needed to determine the principal aerodynamic performance parameters of such a vehicle. Therefore most of the preliminary design effort was concentrated around developing a balance configuration in which the coupling between these components is minimal.

Measurement of the remaining components (side force, yawing moment and rolling moment) was also an important design criterion, because the interaction between all six components determines the overall dynamic behaviour of the balance. Therefore the measurement of side force, yawing moment and rolling moment is necessary to quantify their effects on the principal balance outputs (lift force, drag force and the pitching moment). It can also be used to improve the accuracy to which the principal balance outputs are measured.

The balance was designed for use over a range of incidence angles up to 50°. This meant that the balance had to be mounted internally within the model and the connection to the supporting stress bar had to be in the base region of the model. This arrangement is generally considered the most flexible in terms of aerodynamic testing as it minimizes the flow field interference caused by the supporting stress bar.

A further constraint on the balance was the available size of the wind tunnel test section (refer to Fig. 3). To permit the balance to be used over a range of incidence angles the length of the supporting stress bar had to be limited. In previous designs [2,3] the force balance/model was supported in the test section by a long supporting stress bar suspended horizontally from flexible steel wires. This arrangement provides a *free-end* condition which is useful in both calibration and experiments as it can be modelled accurately. For the present balance a *fixed-end* condition for the supporting stress bar was necessary to produce measurable strain levels in the supporting stress bar. With an impedance mismatch between the model and the supporting stress bar, a number of stress wave reflections within the model is required for the strain level to rise in the supporting stress bar. If the supporting stress bar is shorter than or of similar length to the length of the model and has a free end, a compressive wave (due to a drag force on the model) will be reflected from the free end as a tensile wave, thus sending the level of stress in the bar back towards zero and causing the complete model and balance arrangement to accelerate. A fixed-end condition with a short supporting stress bar enables the level of stress to rise to measurable levels during the test period. The fixed-end condition is produced by connecting the end of the supporting stress bar to a relatively large mass, rigidly mounted in the test section. This serves to reflect stress waves back from the end of the supporting stress bar enabling measurable strain levels to be developed in the force balance. To simplify the FE modelling a fixed-end condition was applied by fully constraining the displacements of nodes at the end of the stress bar. This will result in some differences from the physical model which has the end of the stress bar connected to a large mass. The minor differences

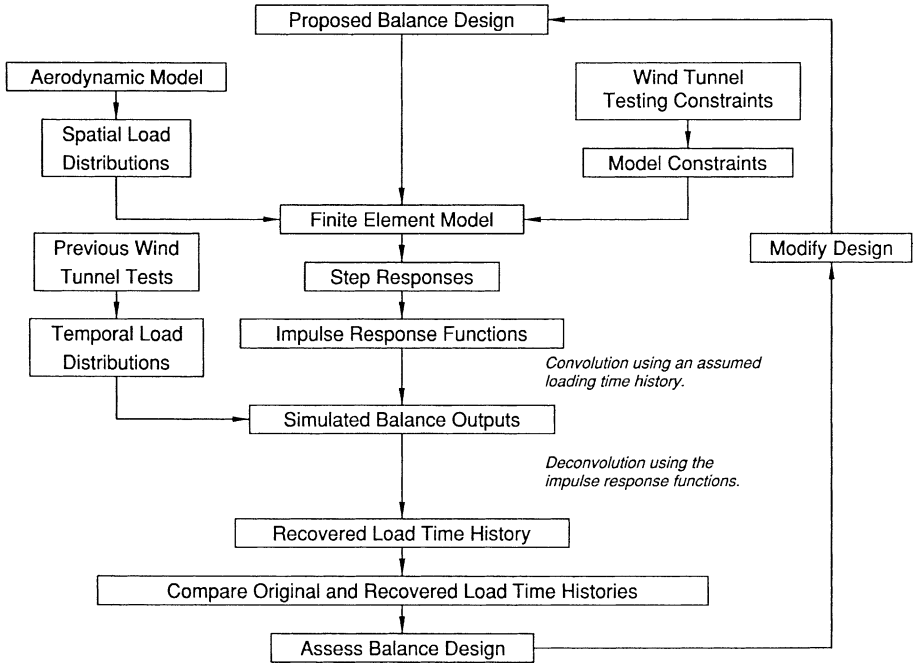

Fig. 4. Methodology used in the design of a stress wave force balance.

resulting from this do not warrant the additional complexity of modelling the large mass and its connection to the tunnel.

7. Design methodology

A summary of the procedure used in the design of the six component balance is illustrated in Fig. 4. The aerodynamic modelling and finite element modelling were used to determine the impulse response functions as described in Sections 3 and 4. In the present six component balance a total of 36 impulse responses was used. Previous testing in the wind tunnel enabled an estimate of the temporal loading distribution to be made. Together with the relative magnitude of load components the temporal loading distribution was used to predict the balance output signals as described in Section 5. Deconvolution then enabled comparison of the recovered loads (in both magnitude and time history) with the original loads. The results of these simulations were then used to guide design refinements and the procedure could be repeated.

This technique was used extensively throughout the design process to help quantify the effect of changes in the balance geometry, loading distribution and the balance support configuration. Additionally, the individual balance step responses were examined to further assess the effects of design alterations on the dynamic response of the balance.

8. Development of balance configurations

Initially many different balance configurations were investigated using the methodology outlined in Section 7. The analysis of these designs provided insight into the dynamic behaviour of the different arrangements and the effects of different geometric features. Some of the general design principles established from this investigation are discussed below.

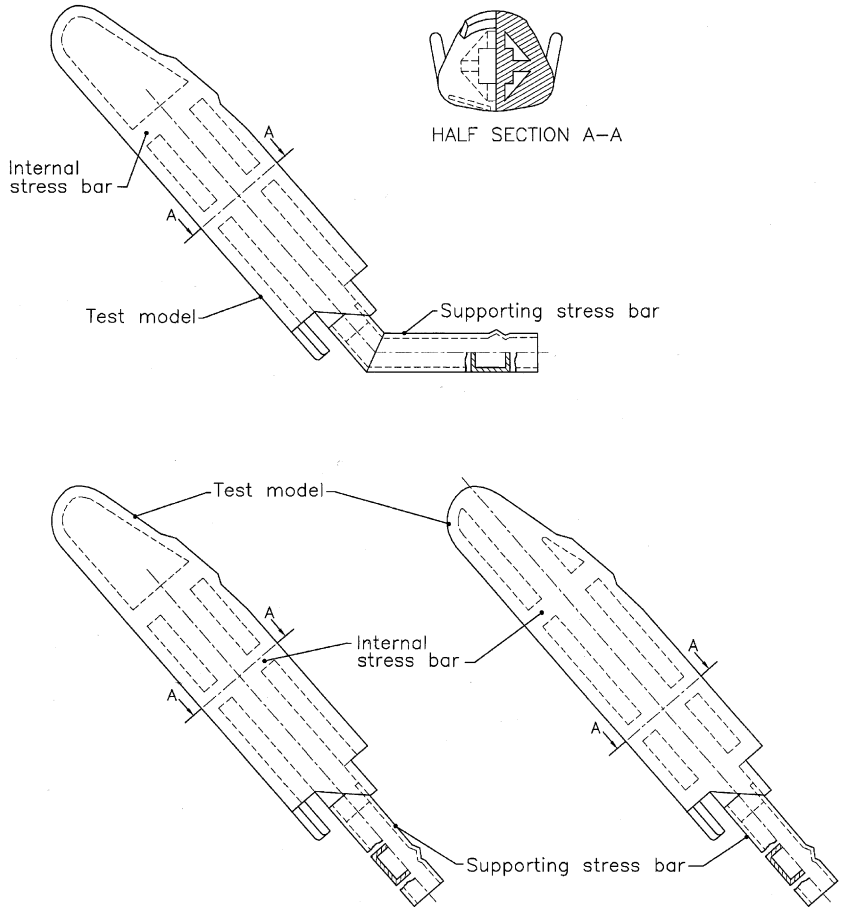

Fig. 5. A schematic representation of three balance designs used in establishing some basic design principles.

Three of the initial balance configurations are illustrated schematically in Fig. 5. These balances were designed to satisfy the constraints discussed in Section 6. All the designs consist essentially of two cruciforms attached to a central bar which extends through the base of the model to form the supporting stress bar. The short bars within the cruciforms are stress bars which are rigidly connected to the inside of the model. The balance outputs for these designs were obtained from axial strain measurements in the eight short stress bars. Additional outputs were taken from axial and shear strain measurements on the supporting stress bar remote from the model connection. This provided 12 strain outputs which were combined to form the six balance outputs which respond primarily to axial, normal and side forces, and rolling, pitching and yawing moments.

The effect of symmetry in the balance geometry was found to be important in all the balance designs. This is because decoupling of force and moment components relies on the similarity of the individual balance output time histories. For example the drag force output, which is measured principally in the supporting stress bar, also relies on symmetrical response from the internal stress bars to remain decoupled from a lift force input. Symmetry of the supporting stress bar, with respect to the measured force and moment components, was also found to influence the performance of balance designs. For example the asymmetry of the supporting stress bar for the design illustrated in Fig. 5(a) caused strong coupling between the output components of the balance and was rejected in favour of the arrangement shown in Fig. 5(b) and (c).

Large differences in the relative stiffness of sections within either the model or the balance can produce vibrational modes which tend to dominate the frequency response. These lower frequency modes often suppress the transmission of higher frequency components between the model and the force balance. This causes problems in the deconvolution of such signals as there may be insufficient frequency content to permit full recovery of the original signal from the balance response. These low frequency vibrational modes occurred in the supporting stress bar and the walls of the model.

The distribution of stress within the internal stress bars was also an important consideration in evaluating proposed balance designs. For the design illustrated in Fig. 5(b) the distribution of stress across the rear bars

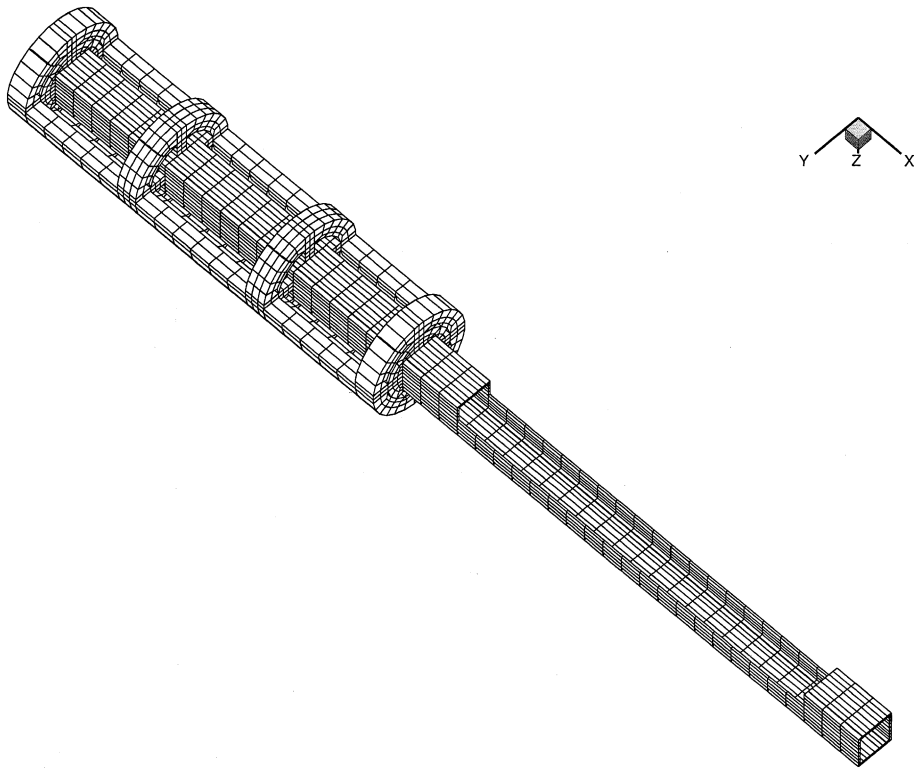

Fig. 6. A finite element mesh of a preliminary force balance design. Note: Sections of the mesh have been removed to reveal internal details of the force balance.

was large. Since the final balance would require instrumentation which relied on bending compensation to achieve accurate measurements, the large variation of stress across the rear bars made the placement of sensing elements very critical. Since the bars would physically be only about 8 mm long and the smallest semi-conductor strain gauges available were about 2 mm long, any error in placement of the gauges could result in unwanted sensitivity to bending strains. This could cause a difference in performance of the physical balance from that of the simulated balance. To avoid this the central bar was extended so it connected into the front of the model and the base of the model was filled in to form another connection to the central bar. These modifications are illustrated in Fig. 5(c) and were found to minimize the stress variation within the internal bars.

These design aspects were incorporated into the development of a preliminary FE model. This model was reasonably simple and permitted optimization of the force balance performance through modification to the internal geometry.

9. Balance refinement

A simplified solid FE model of the balance geometry shown in Fig. 5(c) was made for further investigations. The FE model was based on a cylinder of the same aspect ratio as the HYFLEX vehicle. The FE model of this design is illustrated in Fig. 6.

After consideration of different model materials aluminium was selected because it has a high elastic wave speed and low internal damping. The FE model was fully constrained at the end of the stress bar remote from the test model. This reproduced the *fixed-end* condition discussed in Section 6. The majority of the loads were applied to the model surface as pressures which were initially distributed uniformly over the model to simplify the modelling. The rolling moment was applied using a series of point loads around the circumference of the model at four locations along the major axis. The Newtonian aerodynamic model was used to determine the relative magnitudes of each force and moment component (refer to Section 3).

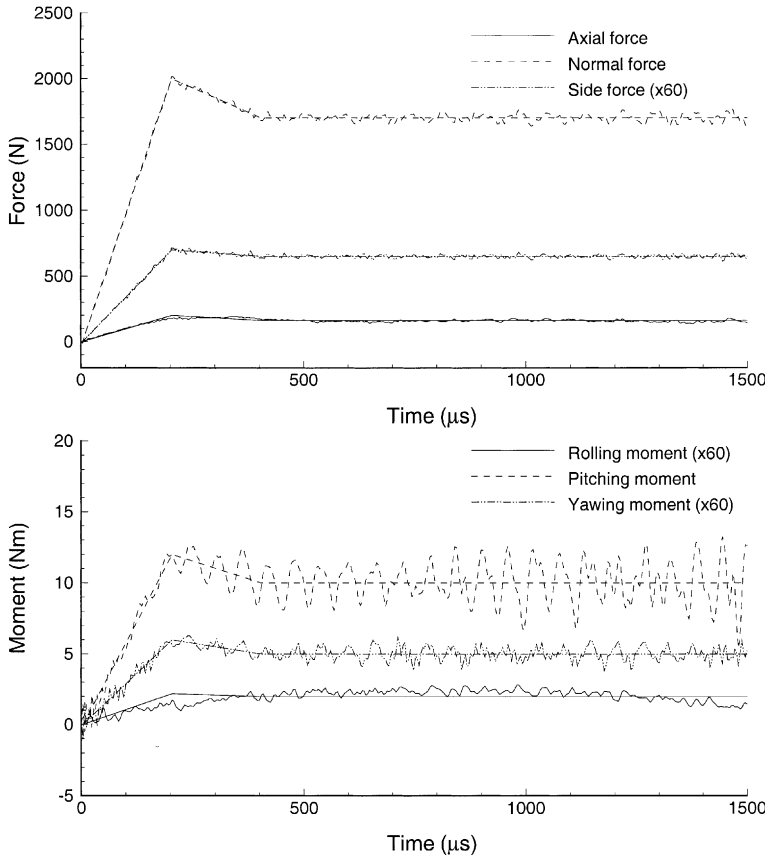

Fig. 7. Original and recovered loads for all six force and moment components obtained from the preliminary FE model. Note: The side force and yawing moment signals have been scaled by a factor of 60 for illustration purposes.

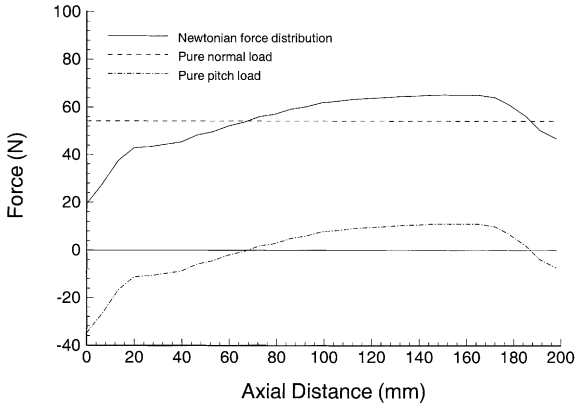

Fig. 8. Distribution of loading used to produced pure normal force and pure pitching moment loadings.

The dynamic response of the balance was evaluated according the procedure discussed in Section 7. Fig. 7 shows a comparison between the original and recovered load time histories for the six force and moment components. Note that the side force, yawing moment and rolling moment signals are smaller in magnitude than the other components and have been scaled for illustration purposes. Fig. 7 demonstrates good signal recovery from all the force and moment components, apart from the rolling moment. Measurement of the rolling moment is difficult because the response time of this component is relatively long. This is due to the low torsional stiffness associated with the supporting stress bar, but it is difficult to increase torsional stiffness in the present arrangement without adversely reducing the axial strain level.

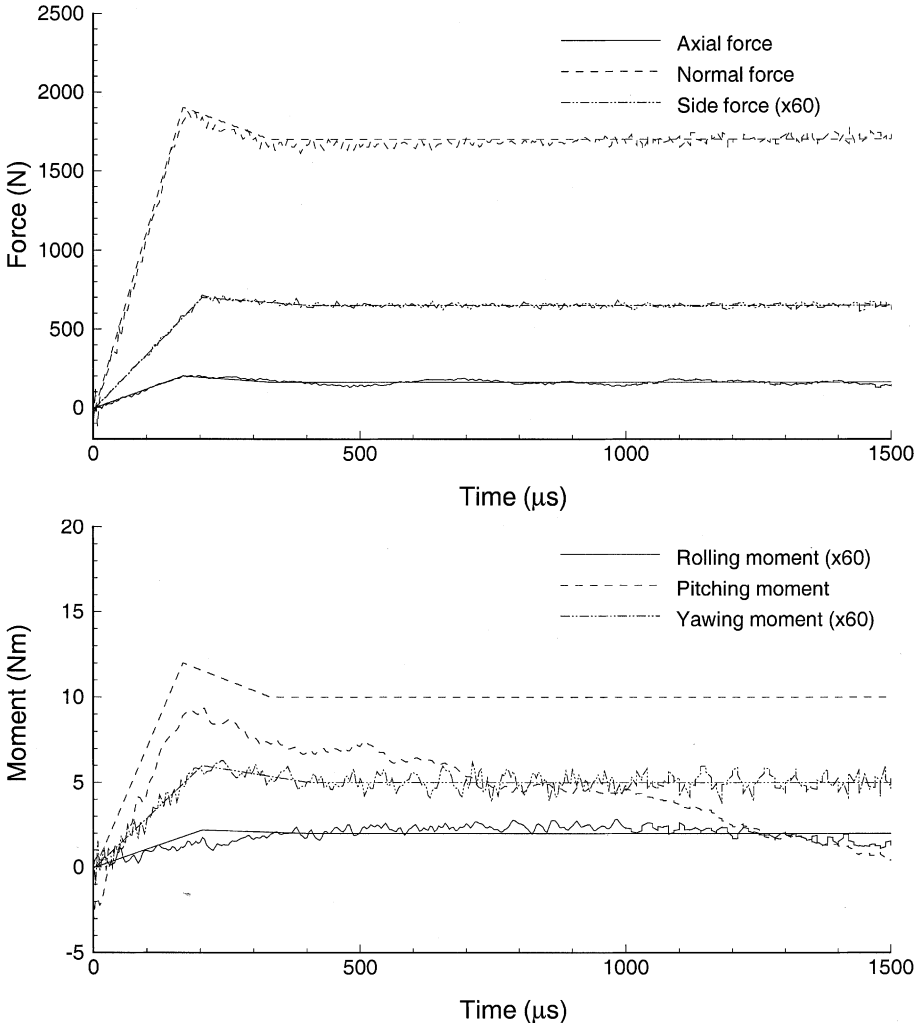

Fig. 9. Original and recovered loads for all six force and moment components subject to the Newtonian loading distribution.

The performance of the balance design was further tested by distributing the loads according to the Newtonian distribution (refer to Fig. 2). The normal force component was calculated to produce the same net normal force as the Newtonian distribution. The pitching moment component was then the difference between this pure normal distribution and the Newtonian distribution of normal force. The distribution of these loads is illustrated in Fig. 8 where the normal force and pitching moment loads are plotted in terms of the axial position along the model. Since the axial force was concentrated around the nose of the model no change was made to the axial force distribution. The side force, yawing moment and rolling moment loads were also unchanged as their distributions were less significant.

The Newtonian distribution of loading was found to produce stronger coupling between the normal force and pitching moment outputs. This resulted in poor signal recovery of the pitching moment. This effect is illustrated in Fig. 9 by the discrepancy in original and recovered pitching moment signals. Recovery of the other force and moment components is still acceptable.

To overcome the pitching moment problem a variety of modifications to the force balance configuration were considered. These modifications included altering the position of the internal stress bars, changing the distribution of mass within the model, reducing the length of the stress bar and examining different output locations and combinations. The most effective modification was changing the position of the force measuring bars. This was found to reduce the coupling between the normal force and pitching moment components and therefore improve signal recovery. Reducing the length of the stress bar also improved the decoupling as the dominance of low frequency oscillations within the balance/model is reduced. Subject to these design changes a new FE model, which incorporated the external geometry of the HYFLEX vehicle, was developed.

10. Final balance design

The final balance design, illustrated in Fig. 10 by the FE model, incorporated the improved balance design into the external geometry of HYFLEX. Only minor features, such as the small winglets and the tail flaps, were omitted to reduce unnecessary model complexity. The internal geometry of the previous design was preserved as far as possible, however some asymmetry resulted from the tapered fore-body.

The new FE model was constrained in the same way as the preliminary model and the loads were applied as pressures to the model surface according to the Newtonian distribution. The original and recovered load time histories for this balance design are given in Fig. 11. These results demonstrate good signal recovery for all the force and moment components, apart from the rolling moment. The results also suggest that the present balance design will be capable of measuring the aerodynamic forces and moments produced by this model in a shock tunnel facility where the loading time history resembles the assumed original loading time history.

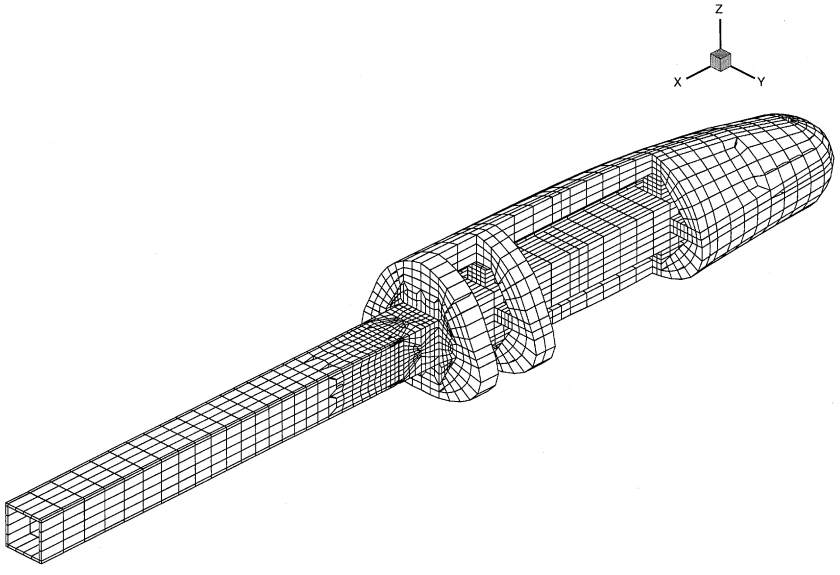

Fig. 10. A refined finite element model of the final balance design incorporated into the proposed shock tunnel test model. Note: Sections of the mesh have been removed to reveal internal details of the force balance.

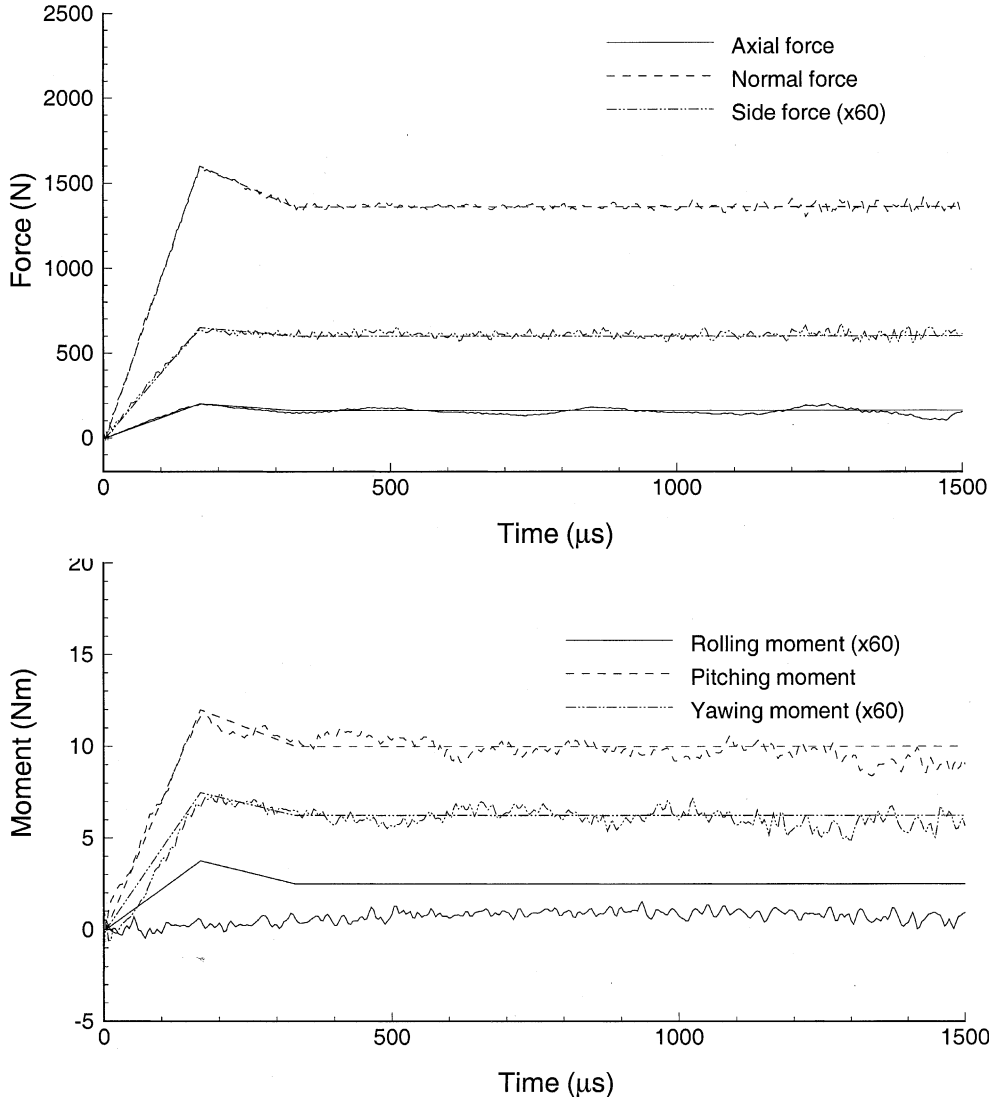

Fig. 11. Original and recovered loads for all six force and moment components.

11. Sensitivity to loading distribution

The sensitivity of the balance to the predicted loading distribution was investigated because the Newtonian loading distribution was only an approximation which did not account for a variety of flow effects. From the earlier assessments of design modifications the pitching moment component was found to be the most sensitive to changes in the loading distribution. Therefore the performance of the balance was examined for a variety of different pitching moment distributions.

A series of alternative pitching moment distributions was calculated to produce a pure moment load of the same magnitude as the Newtonian loading prediction. The new pitching moment distributions then were applied to the FE model and a new set of step responses determined. Impulse response functions were then generated from these new step responses and were used to form simulated balance outputs. These simulated outputs were then deconvolved using the original impulse response functions obtained from the Newtonian distribution of loading.

Results from a series of these tests demonstrated that the individual pitching moment load could be perturbed by an average of 20%, from the original Newtonian distribution, with the difference between the true and recovered pitching moment signals being approximately 5%. This corresponds to an error in the location of the

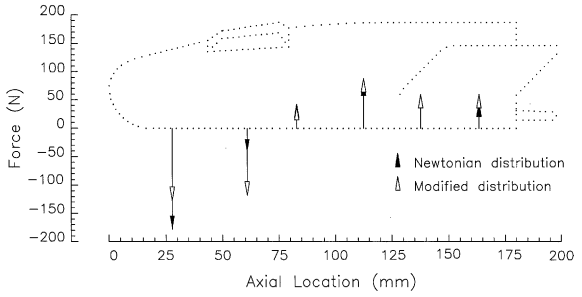

Fig. 12. A discretised Newtonian and modified distribution of pitching moment loading used to examine the balance sensitivity to pitching moment distribution. Note: Each distribution produces zero net normal force and the same total pitching moment.

centre of pressure of approximately 0.5% of the model length. An example of two test loading distributions is shown in Fig. 12. Both produce the same net normal force and pitching moment. While this is not a rigorous treatment of load distribution sensitivity, it demonstrates that for small changes in the pitching moment distribution, the balance is capable of accurately resolving the magnitude of applied pitching moment.

12. Summary

A combination of modelling techniques has been used in conjunction with a design methodology to simulate the performance of a six component stress wave force balance. The modelling techniques enabled a variety of design features to be investigated and their effects on the balance performance quantified. This enabled the measurement capability of the design to be optimized for the loading time histories expected in a reflected shock tunnel facility. The final design incorporated the complex geometry of a typical hypersonic test model vehicle. The performance of this design suggests it should be capable of measuring three force and two moment components, but that it is unsuitable for accurate measurement of rolling moment.

Acknowledgements

The authors gratefully acknowledge the financial support of the Australian Research Council and the Australian Space Office. The FE simulations were run at The University of Queensland High Performance Computing Facility. Thanks also go to Kevin Austin for his assistance in the modified-Newtonian calculations.

References

[1] Rae WH, Pope A. Low-speed wind tunnel testing. New York: Wiley; 1984.
[2] Sanderson SR, Simmons JM. Drag balance for hypervelocity impulse facilities. AIAA J 1991;29(1):2185–91.
[3] Daniel WJT, Mee DJ. Finite element modelling of a three-component force balance for hypersonic flows. Comput Struct 1995;54(1):35–48.
[4] Mee DJ, Daniel WJT, Simmons JM. Three-component force balance for flows of millisecond duration. AIAA J 1996;34(3):590–5.
[5] Shirouzu M, Wantanabe S, Suzuki H, Yamamoto M, Morito T. A quick report of the hypersonic flight experiment, HYFLEX. 20th International Symposium on Space Technology and Science, Gifu, Japan, 19–25 May, 1996.
[6] Davies R.M. A critical study of the hopkinson pressure bar. Philos Trans Royal Soc London 1948;240 (Series A):375-457.
[7] Mee DJ. HYFORCE computer program for numerical deconvolution. Software, Department of Mechanical Engineering, The University of Queensland, 1998.
[8] Prost R, Goutte R. Discrete constrained iterative deconvolution algorithms with optimized rate convergence. Signal Process 1984;7(3):209–30.
[9] Anderson JD. Hypersonic and high temperature gas dynamics. New York: McGraw Hill; 1989.
[10] Smith AL, Johnston IA, Austin KJ. Comparison of numerical and experimental drag measurement in hypervelocity flow. Aeronaut J 1996;100(999):473–80.